Fuel 392 (2025) 134837

Contents lists available at ScienceDirect

Fuel

journal homepage: www.elsevier.com/locate/jfue

Full length article

Efficient and durable system design for ammonia-fueled solid oxide fuel cells using multiscale multiphysics modeling approach

Arash Nemati [a,*], Hossein Nami [b], Javid Beyrami [a], Rafael Nogueira Nakashima [a], Henrik Lund Frandsen [a]

[a] Department of Energy Conversion and Storage, Technical University of Denmark, Fysikvej, DK-2800 Kgs. Lyngby, Denmark
[b] SDU Life Cycle Engineering, Department of Green Technology, University of Southern Denmark, Campusvej 55, Odense M, 5230, Denmark

HIGHLIGHTS

- A multiscale multiphysics modeling approach for ammonia-fueled SOFC system design
- Different system configurations are designed including AOR and ammonia pre-cracking
- Inlet temperature and air flow rate should be controlled for different configurations
- Anode off-gas recirculation (AOR) showed a significant improvement in efficiency
- A high ratio of ammonia pre-cracking (~80–90%) is required to avoid nitriding

GRAPHICAL ABSTRACT

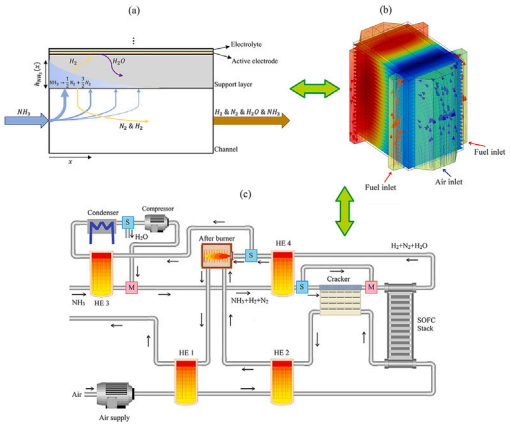

ARTICLE INFO

Keywords:
SOFC
System design
Ammonia fuel
Pre-cracker
Durability
Nitriding

ABSTRACT

It is crucial to consider all of the scales and underlying physics to design a durable and efficient ammonia-fueled SOFC system. Therefore, a novel multiscale multiphysics modeling approach is used in this study as a design tool to investigate various features of ammonia-fueled SOFC systems, stacks, and cells including performance and nitriding degradation. Different system configurations are designed and influence of anode off-gas recirculation (AOR) and ammonia pre-cracking is investigated. Results indicate the impact of the design changes on efficiency and nitriding degradation. Air flow rate and inlet temperature should be controlled for different configurations to keep the temperature of cells in the stacks inside a desired range. Implementing the AOR showed a considerable improvement in efficiency as for 0 %, 50 %, 70 %, and 90 % AOR rates, system efficiencies are around 53 %, 63 %, 70 %, and 75 %, respectively. To avoid nitriding at the given operating conditions, around 90 % external pre-cracking is required. A system with 90 % of pre-cracking and 90 % AOR is selected as the most efficient and durable system configuration, for the technology at hand. Pressure drops in the system components, particularly on the air side, should be minimized to achieve high efficiency in cases with high ammonia pre-cracking ratios.

* Corresponding author.
Email addresses: arnem@dtu.dk (A. Nemati), hlfr@dtu.dk (H.L. Frandsen).

https://doi.org/10.1016/j.fuel.2025.134837
Received 14 October 2024; Received in revised form 13 February 2025; Accepted 20 February 2025
Available online 28 February 2025

1. Introduction

Persistent reliance on carbon-intensive fossil fuels contributes to climate change, accelerating glacier retreat and sea-level rise, thereby creating an urgent need for low-carbon or carbon-free energy solutions [1]. Fuel cells are distinguished as a promising power production technology because of their eco-friendly attributes and high energy efficiency [2]. Solid oxide fuel cells (SOFCs) are a highly promising power generation technology, offering the potential for achieving exceptional electrical efficiency [3]. Moreover, SOFCs can be powered directly by a variety of fuels [4] such as methane, ammonia, and methanol, eliminating the need for expensive separation of carbon-based compounds or nitrogen from hydrogen before entering the fuel cell [5].

Ammonia (NH_3) presents itself as an attractive carbon-free fuel for SOFCs, with benefits like reduced flammability, easier liquefaction, and more straightforward transportation when compared to hydrogen [6,7]. Ammonia can be fed into SOFCs using two methods. It can be directly fed into the SOFC stack, where it undergoes internal cracking inside the nickel layers within the cells. This method is called direct ammonia-fueled SOFC [8,9]. In the other method, which is called pre-cracked ammonia-fueled SOFC, NH_3 is initially cracked into N_2 and H_2 in an external cracker [10,11].

Besides the advantage of SOFC stack cooling due to internal cracking of NH_3 in direct NH_3-fueled SOFCs, presence of ammonia can cause nitriding of the nickel in both the active electrode and the fuel support layer. Nitriding can lead to a degradation in the performance of the SOFC [12]. Nitriding of nickel may cause a change in the morphology of the Nickel/Yttria-Stabilized Zirconia (Ni/YSZ) layers and even cause delamination of the cell during temperature cycling [12]. Nitriding can also occur in other components within the SOFC stack, like interconnects and metal parts. 1000-hour tests were conducted on an SOFC stack fueled directly by ammonia at 750 °C [13]. The tests showed that nitriding occurred on the metallic interconnect on the fuel side, resulting in considerable deformation and the presence of Fe-rich regions on the surface [13]. Therefore, it is important to avoid nitriding formation in the NH_3-fueled SOFCs. Recently, Nemati et al. [14] experimentally investigated Ni nitriding in a direct NH_3-fueled SOFC at the cell level. They also simulated the risk of Ni nitriding and validated their model with experimental data. Their results indicated that the risk of Ni nitriding is more severe at low temperatures less than 750 °C and high ammonia flow rates where ammonia survives and penetrates further along the cell.

In a power production unit, the NH_3-fueled SOFC stack is anticipated to be part of a broader system that includes heat exchangers, air and fuel supply systems, and an external NH_3 cracker. Numerous studies have been carried out on the modeling of NH_3-fueled SOFCs at system-level [15–21]. Cinti et al. [15] conducted experimental tests on hydrogen and ammonia-fueled SOFC stacks and made a 0-dimensional (0-D) thermodynamic model of a system based on their test results. The results showed that the ammonia-fueled SOFC was more efficient than its hydrogen-fueled counterpart. This was due to the cooling effect of endothermic ammonia cracking which reduced energy consumption needed to supply the air flow for SOFC cooling. Rokni [16] performed a comprehensive study on anode off-gas recirculation (AOR) in a SOFC system fed with different fuels using a 0-dimensional model. AOR is a recognized method for improving SOFC performance by reintroducing a portion of the anode exhaust gas into the SOFC. In the analyzed system, anode off-gas was fed into the setup without condensation or steam separation. It was observed that ammonia-fueled systems exhibited lower efficiency compared to standalone SOFC systems, attributed to fuel dilution by steam [16].

Selvam et al. [17] carried out a thermodynamic analysis on an SOFC system designed with 100 % fuel utilization through a dead-end anode (DEA) loop, utilizing a 0D model for the SOFC. The results were compared with those of a conventional SOFC configuration that included an afterburner, showing a 12.17 % enhancement in system efficiency. Quach et al. [18] proposed three ammonia-fueled SOFC systems using a 0-dimensional model for the SOFC stack. Using a water condensation system for recirculation led to an increase in system efficiency to 67.4 % by recycling hydrogen-rich gas. Sun et al. [19] employed 0D steady-state models for the SOFC stack and its associated balance of plant (BOP) components to evaluate a kW-level ammonia-fueled system. They concluded that anode off-gas recirculation with steam separation considerably improves the net electrical efficiency. They concluded that by using additional external cooling water, the stack fuel utilization range and the net electricity efficiency of the system could be extended to 0.58–0.80 and 51.84–57.15 %, respectively.

Cinti et al. [20] using a 0-D model investigated three strategies to improve ammonia-fed system performances: (1) the introduction of an additional stack to distribute the power i.e. power rating, (2) the evaluation of the anode off gases recirculation and (3) the use of the off gases to operate a cascade stack (re-powering), where the anode flue gas is recuperated. They concluded that by combining the three proposed solutions, the net efficiency can be enhanced from 52.1 % to 66 %, while the required heat exchanger surface area can be reduced by 67 % compared to the baseline design, which does not incorporate any of these strategies. Quach et al. [21] introduced an ammonia-fueled cascade recirculation system featuring two stacks arranged in series, along with an anode off-gas recirculation setup aimed at enhancing system efficiency. They used a 0-D model of SOFC and compared the two system configurations. The findings indicated that the system's electrical efficiency reached 67.78 % for the cascade-only configuration and 68.80 % for the cascade recirculation setup. They also evaluated the efficiency of their proposed systems under varying fuel utilization rates, ranging from 66 % to 82 %. They observed that reducing fuel utilization improved the electrical efficiency of their designed systems.

Additionally, a few studies have adopted alternative approaches to stack modeling compared to the above-mentioned literature. Wehrle et al. [22] adopted a multi-scale modeling approach to investigate a hybrid solid oxide fuel cell–gas turbine system powered by ammonia. Their methodology included an elementary kinetic model for ammonia cracking and a 3D simulation of a pressurized SOFC stack. The model was validated using experimental data from a button cell operating between 500 and 675 °C. They identified a notable performance disparity between H_2-fueled and direct NH_3-fueled cells, particularly at temperatures below 600 °C, due to the slow decomposition kinetics of NH_3. They also concluded that pressurizing can enhance the cell power considerably. However, this study did not address nitriding issues or explore potential system configurations. Cheng et al. [4] used mapping of current, reaction heat, temperature, and species feeds to model a commercial 700 W cross-channel SOFC stack with H_2, NH_3, and reformed CH_4 fuels. They coupled their stack mapping modeling approach with a system model and calculated the system efficiency of 52.60 %, 44.74 %, and 42.63 % for NH_3, H_2, and reformed CH_4 fuels, respectively.

Numerical models are essential for gaining a deeper understanding of the complex phenomena involved in SOFCs. These models enable researchers to simulate and analyze diverse operating conditions, investigate the complex processes within the cell, and forecast its performance across various scenarios, often challenging or impossible to measure directly. Numerical simulations help in understanding the underlying physics, optimizing cell, stack, and system design, and exploring novel approaches for enhancing the efficiency and durability of NH_3-fueled SOFC systems.

In the study of NH_3-fueled SOFC systems, 0-D models are commonly used in the literature. Existing 1-D and 2-D models usually focus solely on the active area of the SOFC. These modeling approaches and assumptions can lead to possible deviations from real-world conditions. For example, when evaluating a temperature range (e.g., 700–800 °C), the SOFC's inlet temperature is often assumed to be lower bound (700 °C) of the range, with a linear temperature gradient assumed within the stack [18,23,24]. Additionally, the outlet temperature is often assumed

to be the upper bound of the range (i.e., 800 °C), which may be inaccurate, particularly in scenarios involving heat transfer to the ambient [25]. This assumption may result in inaccuracies in the system's thermal balance. The temperature distribution is not linear in reality; rather, the inlet, outlet, and overall temperature profiles are significantly affected by the operating conditions in direct NH_3-fueled SOFCs. In some of the commercial stacks, the fuel manifolds are located on the sides of the stack which may lead to non-uniformities in fuel distribution, current density, and other parameters in x and z directions [25] (y is the flow direction along the cell). These non-uniformities can be captured by the 3D model. The 3D model can also be used to simulate cross-flow stack configurations, which cannot be accurately represented by 1D or 2D models. Moreover, 3D multiphysics simulations can serve as a valuable and accurate tool for predicting thermal stresses and simulating potential fractures in the cells and the sealing, which is beyond the scope of this paper but will be explored in future research. This approach also allows for more precise calculation of pressure drops within the SOFC stack, unlike simplified models. Also, degradation over the lifetime of the stack due to nickel coarsening, chromium poisoning, and oxidation of the interconnect is a locale phenomenon and varies along the height of the stack which can be captured by 3D multiphysics model [26]. Therefore, the integration of the 3D model with the system model used in the current study offers significant advantages compared to previous modeling approaches.

Based on the reviewed literature, there are few investigations on the coupling of system-level modeling and detailed 3-D modeling of the SOFC stack considering air and fuel manifolds and all other details in the 3-D model. Integrating detailed three-dimensional modeling of the SOFC stack with system-level modeling provides a more accurate and holistic understanding of various elements of NH_3-fueled SOFC systems, including nitriding degradation, which is currently not addressed in the literature concerning the design of these systems. This approach facilitates the design of various system configurations to address potential drawbacks of ammonia-fueled SOFCs, ultimately achieving an efficient and durable system design for an ammonia-fueled SOFC system.

Therefore, this paper employs a novel multiscale approach that integrates three-dimensional multiphysics modeling of stacks with system-level modeling. The developed model is employed to design different system configurations and investigate possible local nitriding in the system. Different system configurations are designed with and without AOR and ammonia external pre-cracking. The objective is to study the impact of the design choices on the performance and nitriding degradation of SOFC systems to guide where to focus further research on materials for the system components. These configurations are then compared based on their efficiency and durability. Different control approaches, including the variation of air flow rate and inlet temperature, are investigated to keep the cell temperature within the targeted range for different configurations. Consequently, two sensitivity analyses are conducted on the effects of pressure drops and air-side inlet temperature on the performance of the system.

The structure of the paper is as follows: the next section outlines the modeling approach and the implemented numerical models. In the results section, the efficiency and operating conditions of different system configurations are initially investigated. Afterward, the effect of steam content in anode off-gas recirculation is investigated on the system performance. Then, the risk of nitriding degradation is examined for the designed configurations. Finally, sensitivity analyses are carried out on the system performance of the selected configuration. The paper concludes by summarizing the key findings and insights.

2. Numerical modeling

This section presents an explanation of the numerical models and methodologies employed in the present study. The organization of this section is as follows:

- Section 2.1: explains the nickel and steel nitriding risk calculation.
- Section 2.2: introduces the model for stack level.
- Section 2.3: describes the model for system level.

All simulation levels are ultimately integrated into a multi-scale model, enabling the assessment of system performance while simultaneously evaluating nitriding criteria at different locations within the cells and across various points in the stack under specific conditions [25]. NH_3 cracking rate inside the Ni–YSZ layers and the corresponding heat sink originating from endothermal NH_3 cracking are explained in ref. [28] and and validated in Section A1 in the supplementary material.

$$R_{crack}^{Ni-YSZ} = 98.4 S_{Ni-pore} exp\left(-\frac{E}{RT}\right) P_{NH_3}^{0.69} (P_{H_2} + 750)^{-0.39} \quad (1)$$

where, R_{crack}^{Ni-YSZ} is the ammonia cracking rate in Ni–YSZ layers in [mol/m^{3}s], $S_{Ni-pore}$ is the Ni-pore contact area density in [μm^2/μm^3], E is the activation energy equal to 1.2×10^5 in [kJ/mol], P_{NH_3} and P_{H_2} are the partial pressures of ammonia and hydrogen in [Pa], respectively. It is assumed that there is no cracking of ammonia on the steel parts.

Fig. 1 illustrates a schematic of the multiscale multiphysics modeling concept for NH_3-fueled SOFCs. This figure illustrates the various levels of the model, including cell, level, and system level. Details of each level will be explained in the following sections.

2.1. Nitriding risk (potential)

Nitriding has been demonstrated to potentially cause damage to layers containing nickel [12,29] and metal components [13] in direct NH_3-fueled SOFCs. According to the customized Lehrer diagram for nickel [30], two phases exist in the nickel-rich area of the Ni–N. The two phases are the Face Centered Cubic (FCC) phase and the Ni_3N phase, which has a Hexagonal Close Packed (HCP) structure [31]. Initially, nitrogen dissolves in pure Ni to form the FCC solid solution, followed by the formation of the HCP phase as the nitrogen concentration increases. The HCP phase is unstable and can lead to the formation of cavities in the attacked metallic surfaces. The repetitive nitriding–reduction cycles result in volume changes (expansion and contraction) that can lead to formation of cavities in the anode. Over time, these cavities may merge, leading to leaks that are harmful to the stack.

The nitriding risk, also called nitriding potential (K_n), is the equilibrium fraction of the nitriding reaction [30]:

$$K_n = \frac{x_{NH_3}}{x_{H_2}^{1.5}} \quad (2)$$

where, x_{NH_3} and x_{H_2} are the mole fractions of NH_3 and H_2, respectively. The occurrence of the different nitrite phases is thus related to this parameter. As HCP is critical for the robustness of the system, we name the phase boundary $K_{n,critical}$. The variation of $K_{n,critical}$ ($K_{n,cr}$) is presented in Fig. 2a. The arrows indicate the regions prone to nitriding in this figure. The boundary varies with temperature, and the FCC phase transitions to the HCP phase more easily at elevated temperatures.

To prevent nickel nitriding, the formation of the HCP phase must be avoided. Thus, the safe region to avoid Ni nitriding is the region, where K_n (Eq. (2)) is lower than $K_{n,cr}$:

$$K_n < K_{n,cr} \Rightarrow \frac{K_n}{K_{n,cr}} < 1 \quad (3)$$

The critical nitriding risk ($K_{n,cr}$) for Fe [32], as the primary component of metal parts, is also shown and compared with $K_{n,cr}$ of Ni in Fig. 2b. It is assumed that, in the absence of more detailed studies, the nitriding of metals can be approximated by the nitriding behavior of Fe. The $K_{n,cr}$ for Fe is lower than Ni, especially at temperatures lower than 650 °C, indicating that the likelihood of nitriding is greater on iron surfaces compared to nickel surfaces.

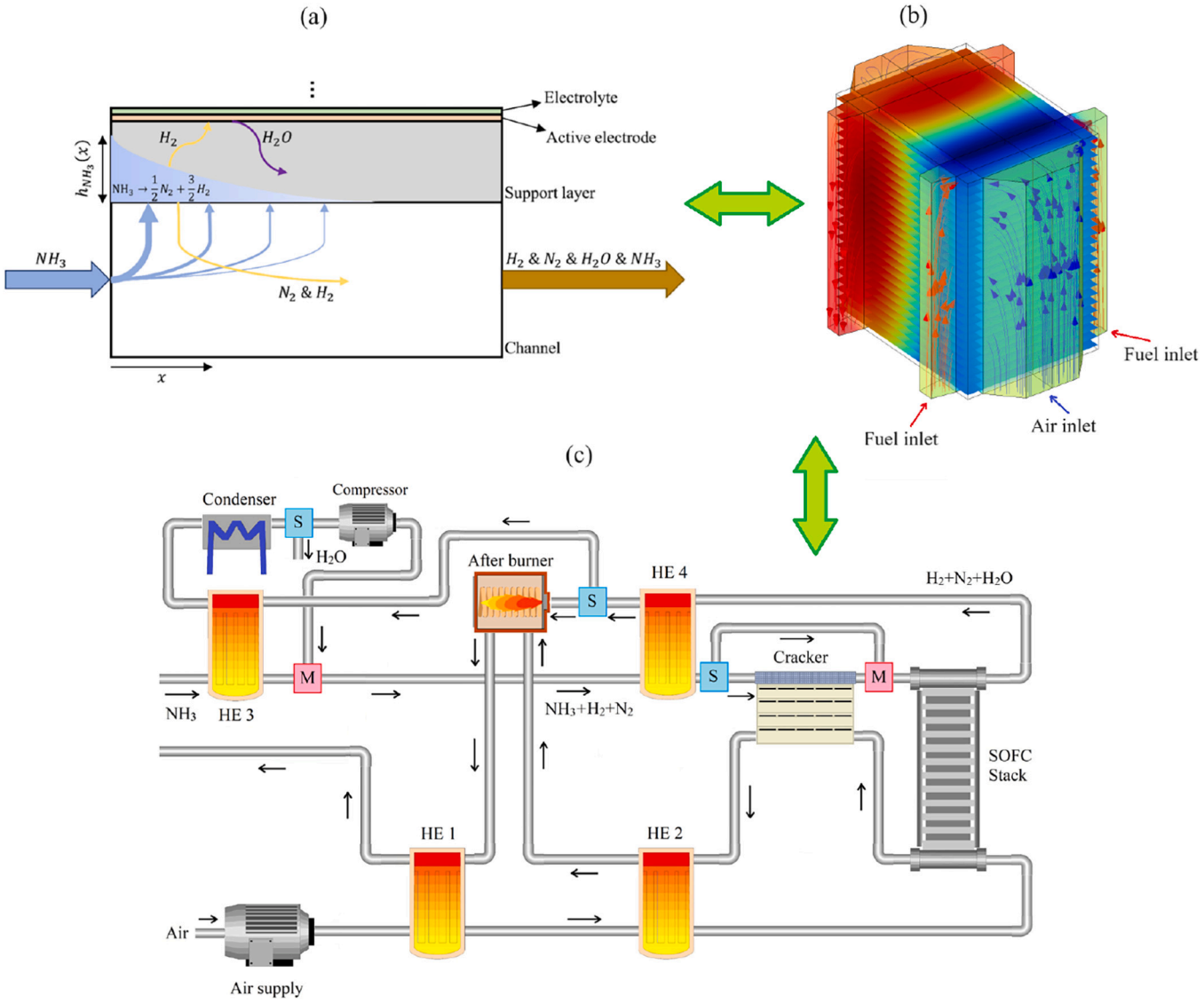

Fig. 1. Schematic of the multiscale multiphysics modeling concept: (a) cell level [27], (b) stack level, and (c) system level. In the schematic of system, heat exchangers are referred to as HE. S and M in the schematics represent splitter and mixer, respectively.

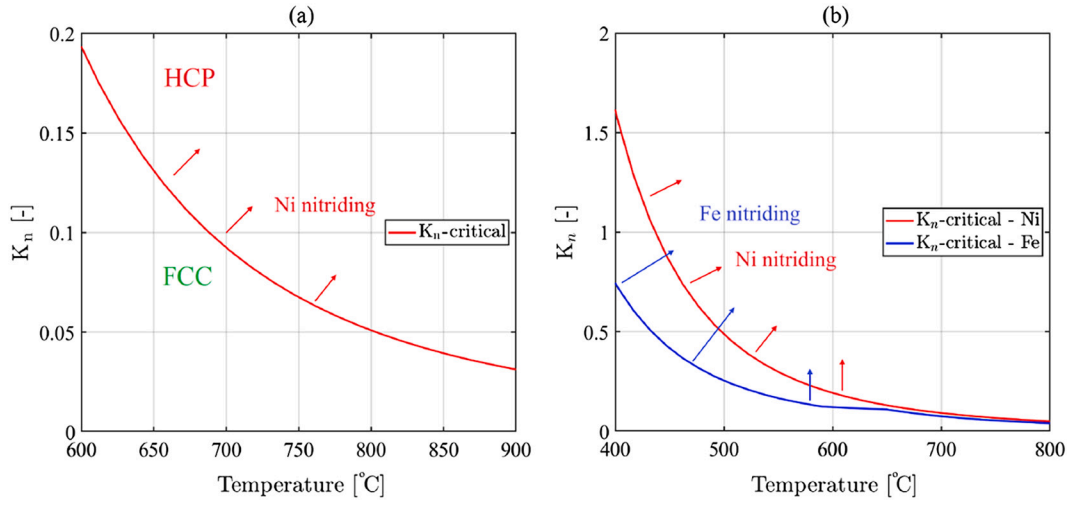

Fig. 2. Variation of critical nitriding risk ($K_{n,cr}$) for (a) Ni and (b) Ni and Fe by temperature [25]. The arrows indicate the regions prone to nitriding in Ni (red arrows) or Fe (blue arrows). (For interpretation of the references to colour in this figure legend, the reader is referred to the web version of this article.)

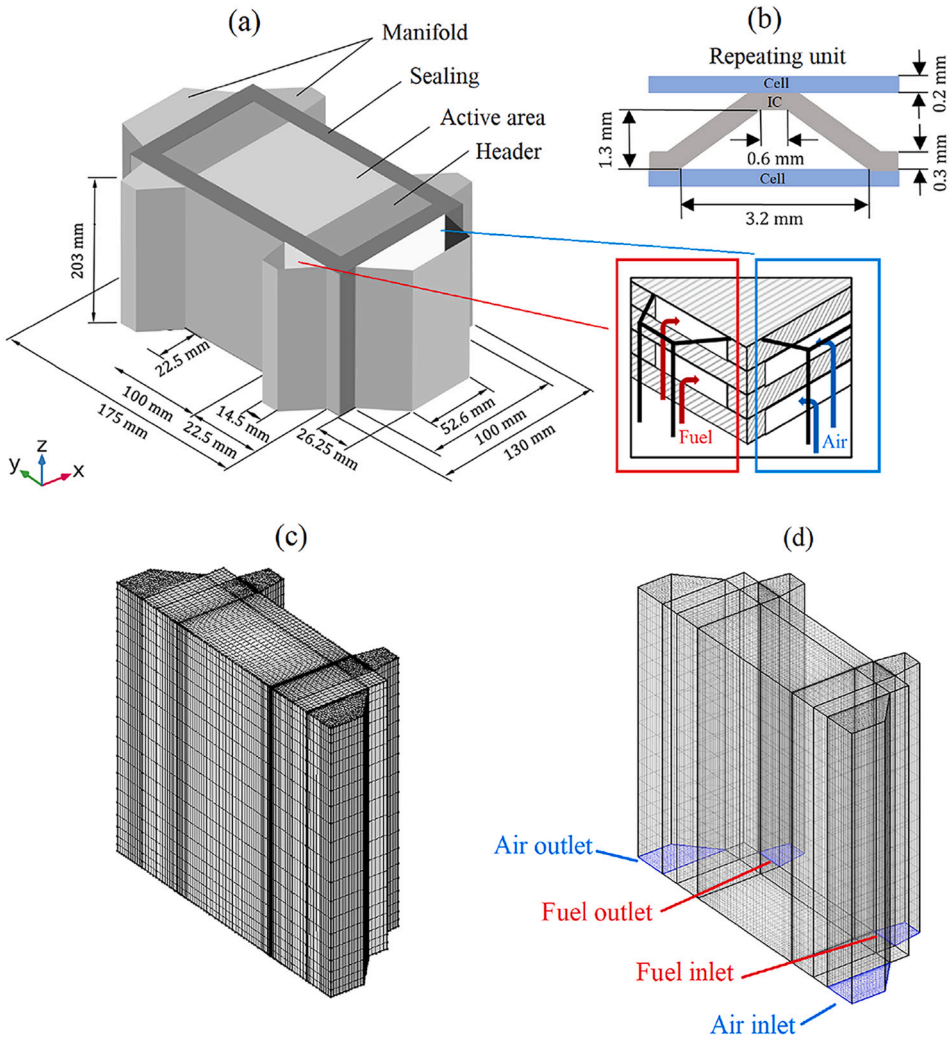

Fig. 3. Schematic of the (a) stack and (b) repeating unit. The mesh and computational domain are shown in (c).

A qualitative validation of the Ni nitriding risk modeling in a direct NH_3-fueled SOFC at the cell level is presented in a previous study [14]. At the stack level, comparing the results of our previous study [25] with a recently published paper on direct ammonia-fueled Elcogen stack [33] proves that the developed model can predict the nitriding at the stack level. Both the developed model and experimental data showed that the stack can tolerate only around 10–15 % of direct ammonia.

2.2. Stack level modeling

Performance studies of the NH_3-fueled SOFC stack are carried out using 3D simulations with COMSOL Multiphysics version 6.1. The 3D geometry of the stack, the computational mesh, and the inlet and outlet of the air and fuel flows are illustrated in Fig. 3. The SOFC stack model utilizes a homogenization approach to solve different physics within the stack [26,27,34]. Detailed explanations of how the homogenization approach is implemented to model voltage, charge transport, mass and momentum transfer, heat transfer, and mechanical stresses in a stack are presented in ref. [34]. This approach provides a significant advantage in computational speed [27] and computational time for a steady-state simulation is around 2–3 minutes on a workstation (Intel(R) Core(TM) i9-9920X CPU @ 3.50 GHz, 12 cores). It is important to highlight that this approach is implemented for all domains except the manifolds [26,35]. The cell characteristics and relevant parameters of the Butler–Volmer (B–V) equation, along with validation of the model at the cell level for hydrogen, pre-cracked, and direct ammonia SOFCs, are provided in Section A2 of the supplementary material. A detailed explanation of the boundary conditions and material parameters for simulating various heat transfer phenomena within the stack, as well as heat transfer from the stack to the ambient environment (e.g., thermal conductivities, insulation thickness, and other relevant parameters), is represented in ref. [34]. The boundary conditions for ammonia-fueled SOFC are explained in ref. [27]. It should be mentioned that radiation is not considered in the modeling of the SOFC stack. The equations and the validation of the stack model are presented in Section A3 in the supplementary material. To save the computational power, the computational domain is limited to half of the stack, as shown in Fig. 3c.

In previous studies [26,35], this modeling approach is utilized to simulate an 18-cell FZJ Mark-F SOFC stack and validate the results with experimental data [36] for hydrogen fuel. Due to the limited availability of experimental data for direct NH_3-fueled SOFC stacks, possibly due to nitriding issues, the stack model has not been specifically validated for NH_3 fuel. However, a recent study [14] employs the same models and equations used in this research within a detailed 3D model at the cell level. A similar cell to the one used in the current study, with the same materials and layer thicknesses, and an active area of 4 cm× 4 cm was tested and modeled in ref. [14]. This model was used to simulate direct and pre-cracked NH_3-fueled SOFC and a very good agreement (less than

3 % error) with experimental data was achieved. Cell characteristics and modeling approach are explained in detail in previous studies [25,27].

The ammonia will crack as it enters the support layer and the fuel electrode. The penetration depths of the ammonia at different locations inside thus have a high influence on the cracking rate. In the homogenized approach this internal reforming is handled through the method developed in [27].

2.3. System level modeling

A multiscale approach, developed in a previous study [25], is employed in this study for system modeling. In this study, detailed 3D modeling of the SOFC stack is combined with a system model, and all relevant equations are solved concurrently using COMSOL. This method enables the application of system-level complexities to the boundaries of the 3D stack model, while the system model benefits from the precision provided by the 3D stack representation [25].

The NH_3-fueled SOFC system is assumed to operate under steady-state conditions. The mass and energy conservation equations for the system components are formulated as follows:

$$\sum \dot{n}_i M_i = \sum \dot{n}_o M_o \tag{4}$$

$$\sum \dot{n}_i h_i + \dot{Q}_{cv} = \sum \dot{n}_o h_o + \dot{W}_{cv} \tag{5}$$

where $\dot{n}$, M, h, $\dot{Q}$, and $\dot{W}$ are mole flow rate, molar mass, specific enthalpy, heat transfer rate, and power, respectively. Indexes i, o, and cv refer to inlet, outlet, and control volume, respectively.

The power of the stack (P_{stack}) and power of the system (P_{system}) are determined using the following equations:

$$P_{stack} = V \times I \tag{6}$$

$$P_{system} = P_{stack} - P_{loss} \tag{7}$$

where V and I are the voltage and current of the SOFC stack, while P_{loss} denotes the power consumed by the fuel and air supply systems.

The energy efficiency of the NH_3-fueled SOFC system is defined as:

$$\eta_I = P_{system}/(\dot{n}_{NH_3} LHV_{NH_3}) \tag{8}$$

where, $\dot{n}_{NH_3}$ denotes the inlet molar flow rate of NH_3 into the system, while LHV_{NH_3} represents the lower heating value of ammonia (18.6 [kJ/mol]).

In order to have a reliable and highly efficient ammonia-fueled SOFC system, four different configurations have been designed and proposed in this section. The schematics of these four ammonia-fueled systems are presented in Fig. 4. The main difference between configurations is whether they include or exclude ammonia cracking and anode off-gas recirculation (AOR).

Table 1 presents a brief description of the different configurations. Configuration 1, the simplest version, lacks ammonia pre-cracking and AOR. It has four heat exchangers for thermal management of the system, an air compressor for air supply, and an afterburner. On the other hand, configuration 4 is the most complex configuration including both ammonia pre-cracking and AOR.

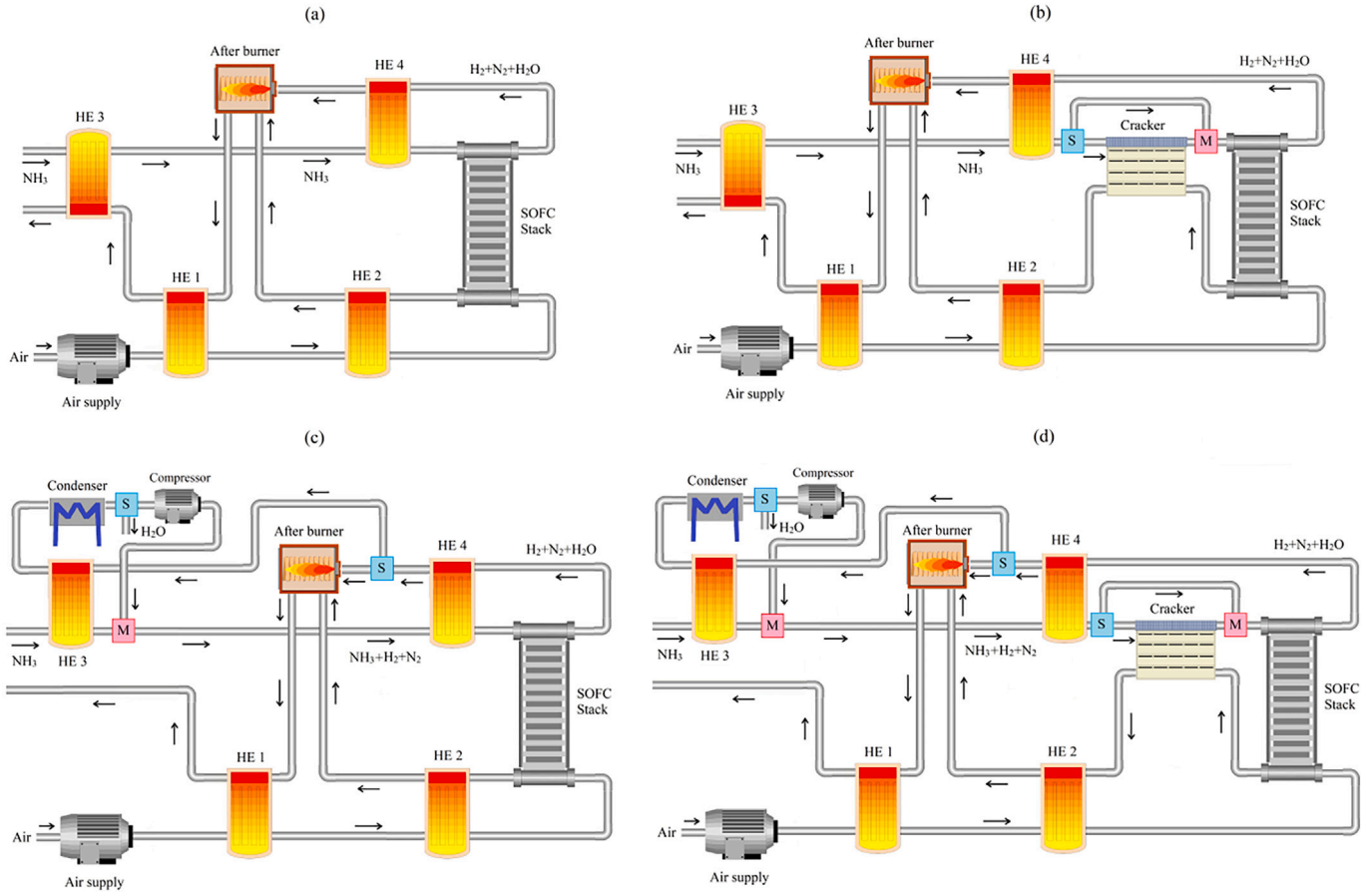

Fig. 4. Schematic of different designed configurations for NH_3-fueled SOFC system, (a) configuration 1, (b) configuration 2, (c) configuration 3, (d) configuration 4. In the schematic, heat exchangers are referred as HE. S and M in the schematics represent splitter and mixer, respectively.

Table 1
Description of different configurations designed for ammonia-fueled SOFC system. Including the process is indicated with a ✓, and not including it is indicated with a ×.

Configuration	Ammonia pre-cracking	Anode off-gas recirculation
Configuration 1	×	×
Configuration 2	✓	×
Configuration 3	×	✓
Configuration 4	✓	✓

Table 2
Assumptions for pressure drops (ΔP) and other parameters and operating conditions utilized in the system modeling.

Parameter	Value [unit]
SOFC fuel utilization factor	70 [%]
SOFC operating current density	0.25 [A/cm^2]
Number of cells and cell active area in the SOFC stack	90 cells 10×10 [cm^2]
Temperature increase within the SOFC stack	100 [°C]
SOFC stack operating temperature range	700–800 [°C]
ΔP in the air heat exchangers on one side	10 [mbar]
ΔP on the air side of the afterburner	10 [mbar]
ΔP on the air side of the cracker	10 [mbar]
ΔP on the fuel side the cracker	5 [mbar]
ΔP in the fuel heat exchangers on one side	5 [mbar]
ΔP on the fuel side of the condenser	5 [mbar]
Maximum effectiveness of heat exchangers	90 [%]
Compressor and blower isentropic efficiency	85 [%]
Minimum condensers temperature	30 [°C]
Ammonia lower heating value	18.6 [kJ mol^{-1}]

The assumptions and operating conditions for various components are summarized in Table 2. The operating conditions of the SOFC stack such as average operating current density (0.25 A/cm^2) and fuel utilization (70 %) are selected based on the recommended values by commercial stack manufacturers [37]. The fuel utilization (FU) is defined based on the equivalent inlet hydrogen and outlet hydrogen as follows:

$$FU = \frac{\dot{n}_{H_2,in} - \dot{n}_{H_2,out}}{\dot{n}_{H_2,in}} \tag{9}$$

where $\dot{n}_{H_2,in}$ is equal to $1.5 \times \dot{n}_{NH_3,in}$ plus $\dot{n}_{H_2,rec}$ (where $\dot{n}_{H_2,rec}$ is the recirculated H_2 is the cases with AOR). The 100 °C temperature increase within the SOFC stack is based on recommended values by SOFC stack manufacturers with similar cell technology (anode supported SOFC). Because of the high pressure in the NH_3 storage tank, no blowers are present on the fuel side of the system. The pressure drop within the SOFC stack is determined using the 3D stack model. The pressure drops in other components are presented in Table 2. These values for pressure drops are assumed configuration 1. The increase or decrease in the pressure drops by changing the flow rates is calculated for other configurations based on the formulation presented in ref. [38].

2.4. Inlet fuel composition definition under anode off-gas recirculation

As all of the ammonia cracked before leaving the SOFC stack under the studied operating temperature (700–800 °C), the anode off-gas contains hydrogen (H_2), nitrogen (N_2), and water vapor (H_2O). For simplification of explanation, it is assumed that H_2O is completely removed by cooling down the anode off-gas in a condenser. However, in reality and also in system analysis in this study, a percentage of H_2O remains (around 4–5 % in this study) in the anode off-gas depending on the condenser temperature. On the other hand, removing N_2 using a membrane requires energy consumption and adds further complexity and cost to the system [17,39]. It is also shown in a previous study [14] that N_2 dilution does not considerably reduce cell performance. There is an accumulated amount of N_2 in the anode off-gas recirculation [14]. To numerically resemble the accumulated N_2 in AOR, Table 3 represents the methodology for the calculation of the accumulated N_2. H_2O is not shown in this table solely for the purpose of simplifying the illustration of the procedure. However, in the calculation of system performance for different configurations, the H_2O content after condensation is also taken into account. This table is represented for the 90 % AOR rate case, and for other AOR rates, the procedure will be the same.

Table 3
Calculation of the inlet fuel composition of the SOFC stack with 90 % AOR rate.

Step	$n_{NH_3,in}$ [mole/s]	$n_{H_2,eq}$ [mole/s]	$n_{N_2,eq}$ [mole/s]	$n_{H_2,out}$ [mole/s]	$n_{H_2,rec}$ [mole/s]	$n_{N_2,rec}$ [mole/s]
1	1	1.5	0.5	0.45	0.405	0.45
2	0.73	1.5	0.815	0.45	0.405	0.733
3	0.73	1.5	1.098	0.45	0.405	0.989
4	0.73	1.5	1.354	0.45	0.405	1.218
5	0.73	1.5	1.583	0.45	0.405	1.425
6	0.73	1.5	1.789	0.45	0.405	1.611
...	...	...	...	...	...	...
65	0.73	1.5	3.646	0.45	0.405	3.281
66	0.73	1.5	3.647	0.45	0.405	3.282

Table 4
Molar flow rates and molar fractions of inlet gas to SOFC stack with 90 % AOR rate based on Table 3.

	NH_3	H_2	N_2
Inlet molar flow rates (mole/s)	0.730	0.405	3.282
Inlet molar fractions (-)	0.165	0.091	0.743

At the start (step 1), it is assumed that 1 mole of NH_3 is fed into the SOFC ($n_{NH_3,in}$). Considering the complete cracking of ammonia, 1 mole of NH_3 is equivalent to 1.5 mole of hydrogen ($n_{H_2,eq}$) and 0.5 mole of nitrogen ($n_{N_2,eq}$) as follows:

$$NH_3 \rightarrow 1.5H_2 + 0.5N_2 \tag{10}$$

Assuming 70 % of hydrogen utilization, the outlet hydrogen ($n_{H_2,out}$) from SOFC is 0.45 mole ($(1-0.7)\times1.5$) and the outlet nitrogen (not shown in Table 3) is the same as the inlet as it is not reacting inside SOFC stack. With an AOR rate of 90 %, the amount of recirculated hydrogen ($n_{H_2,rec}$) and nitrogen ($n_{N_2,rec}$) is calculated by multiplying the outlet values by 0.9:

$$n_{H_2,rec,step1} = 0.45 \times 0.9 = 0.405 \tag{11}$$

$$n_{N_2,rec,step1} = 0.5 \times 0.9 = 0.45 \tag{12}$$

In step 2, to have the same amount of hydrogen as in step 1, i.e. 1.5 mole, the inlet NH_3 is reduced to 0.73 mole, and recirculated N_2 is added to the corresponding amount of N_2 from NH_3 i.e.:

$$0.73 \times 0.5 + 0.45 \rightarrow 0.815 \tag{13}$$

In the next steps, the amount of NH_3 and H_2 remains the same as in step 2 and N_2 continuously increases. The steps are repeated until the difference in $n_{N_2,in}$ is less than 0.001 mole. The values in step 66 are used for the calculation of molar fractions of species at the inlet of the SOFC stack. The molar flow rates of the inlet stream to the SOFC stack and corresponding molar fractions for a case with 90 % AOR rate can be observed in Table 4. Inlet molar flow rates in Table 4 for NH_3, H_2, and N_2 equal $n_{NH_3,in}$, $n_{H_2,rec}$, and $n_{N_2,rec}$ from Table 3, respectively.

It should be mentioned that the model is validated at the cell level for AOR rates of 70 %, and 90 % for a cell with the same materials for AOR rates of 70 % and 90 % in previous study [14].

A similar procedure has been considered in the AOR cases with steam recirculation in Section 3.2, to account for the cumulative amount of steam in the inlet mixture of the SOFC stack.

3. Results and discussion

This section discusses the results obtained from the developed model for different system configurations tailored for the ammonia-fueled SOFC system. This section is structured as follows:

- Section 3.1: presents the operating conditions and performances of different system configurations for ammonia-fueled SOFCs.
- Section 3.2: studies the influence of steam in AOR on the system performance.
- Section 3.3: investigates the nitriding risk for different proposed configurations.
- Section 3.4: represents the sensitivity of the system efficiency to pressure drops.
- Section 3.5: studies the sensitivity of the system efficiency to air side inlet temperature.

3.1. Different configurations for ammonia-fueled SOFC systems

This section offers a comprehensive overview of the operating conditions for all configurations. The schematic of different designed configurations is presented in Fig. 4.

3.1.1. Operating conditions for different system configurations

In all of the configurations, the operating temperature of the NH_3-fueled stack remains within the constrained range of 700–800 °C. The ammonia cracking reaction is an endothermic process. Hence, when NH_3 cracking takes place internally within the SOFC stack, a localized temperature reduction occurs. Therefore, in these cases, the inlet temperature should be higher than 700 °C (the lower bound of the operating range) to ensure that the minimum temperature of the stack remains above 700 °C at the entry of the electrochemically active part of the stack. On the other hand, in the cases with NH_3 pre-cracking, it is imperative to elevate the airflow rate to maintain the maximum temperature of the stack below 800 °C.

Therefore, two controlling strategies are employed in this study to keep the operating temperature of the SOFC stack within the desired range of 700–800 °C. These strategies involve adjusting the inlet temperature and modifying the air flow rate which are represented in Table 5 for the different system configurations. For configuration 3 (see Fig. 4b), three different recirculation rates including 50 %, 70 %, and 90 % are considered.

From Table 5, it can be observed that the highest and lowest inlet temperatures belong to configurations 1 and 4, respectively. Temperature distributions inside the SOFC stack are illustrated in Fig. 5 for the different system configurations. It is important to note that the gas inlet temperature for both the air and fuel sides is assumed to be identical. In configuration 1, where there is no pre-cracking or recirculation, a significant decrease in temperature can be observed as a result of the endothermic cracking of ammonia. In configurations 2 and 4, where a majority of NH_3 is pre-cracked outside the SOFC stack, the temperature rises from the inlet to the outlet due to the exothermic electrochemical reactions occurring within the SOFC stack. In configuration 3, which incorporates AOR, the quantity of inlet ammonia is reduced, and the cracking of ammonia is delayed due to the presence of hydrogen. This leads to lower local temperature reduction compared to configuration 1.

Fig. 5 also illustrates the variation in air temperature along the stack from inlet to outlet across seven different lines in the z-direction for different configurations. As can be seen, all temperatures remain equal to the inlet temperature until approximately −90 mm, where they begin to decrease due to the endothermic cooling effect of ammonia cracking which is more pronounced for configuration 1 (Fig. 5a). The lines close to the upper and lower parts are colder than the lines in the middle of stack due to higher heat transfer. After the initial cooling down, the temperature in the various lines increases from −50 mm to approximately +50 mm, corresponding to the active area of the stack, primarily due to the heat generated by electrochemical reactions and ohmic heating. After passing +50 mm, there is no significant change in temperature as there are no heat sources or heat sinks and gas is passing through the solid parts of the stack. Around +90 mm, the outlet air manifold begins, where air flows from different cells mix, resulting in a temperature variation across the different lines. These temperature profiles along different lines in the z-direction illustrate the potential variation in stack parameters across the z-axis.

By reducing the internal cracking of ammonia, the airflow required to keep the temperature of SOFC stack within the desired range of 700–800 °C is increased. This will affect the system performance as elaborated in the following subsection. The required air flow rate is slightly reduced by increasing the AOR rate (Table 5). However, this contrasts with the reduced endothermic cracking of ammonia due to lower inlet ammonia at higher AOR rates. As it can be seen from Table 3 the fuel flow rate considerably increases by increasing the AOR rate due to accumulated N_2 in the recirculation stream. Also, the inlet temperature reduces by increasing AOR rate the reduced ammonia content, and the lower ammonia cracking rate. Therefore, by increasing the AOR rate, the higher fuel flow rate with lower temperature leads to more cooling and lower required air flow rate for cooling the SOFC stack.

3.1.2. System performance for different system configurations

Table 6 presents the outlet air temperature of the designed system configurations as a source of energy for waste heat recovery, along with the system efficiency, for various configurations. In the configurations incorporating pre-cracking, a higher airflow is required to cool down the stack temperature as the endothermic ammonia cracking reaction is absent inside the SOFC stack. Consequently, the outlet temperature of the system is lower because more energy is required to heat the high inlet air flow rate to the desired temperature for the SOFC stack. From Table 6 it can be observed that the system outlet temperature decreases with the AOR rate increasing. The increase in the AOR rate results in a reduction of the fuel quantity from the anode off-gas that burns in the afterburner. This reduction ultimately leads to a decrease in the outlet temperature of the system.

By comparing the efficiencies, it can be concluded that ammonia pre-cracking leads to a reduction in the system efficiency, since more air flow and power for compression of air are needed as shown in Table 5. It should be mentioned that the presented efficiencies are based on the assumed pressure drops presented in Table 2. In Section 3.4, a sensitivity analysis will be conducted to evaluate the effect of pressure drops on the system efficiency.

It can also be seen that implementing AOR and increasing the AOR rate significantly enhances the efficiency of the system. To attain a system efficiency higher than 70 %, a high AOR rate (80–90 %) is required, considering the pressure drops across the system components. This clarifies the importance of AOR for the designed NH_3-fueled system. It should be mentioned that the calculation of efficiencies for AOR cases is conducted considering the removal of a large amount of H_2O content (~ 95 %) from anode off-gas by a condenser (see Fig. 4). In the following section, influence of removing condenser and keeping all amount of H_2O is investigated on the system performance.

Table 5
Temperature and air flow rate for different configurations. The amount of ammonia pre-cracking and AOR rate are presented in case ID.

Configuration	Case ID	Inlet temperature [°C]	Air flow rate [mol/s]
1	0 % pre-crack, 0 % AOR	750	0.1595
2	80 % pre-crack, 0 % AOR	704	0.2323
3	0 % pre-crack, 50 % AOR	732	0.1651
3	0 % pre-crack, 70 % AOR	724	0.1596
3	0 % pre-crack, 90 % AOR	718	0.1526
4	90 % pre-crack, 90 % AOR	702	0.2358

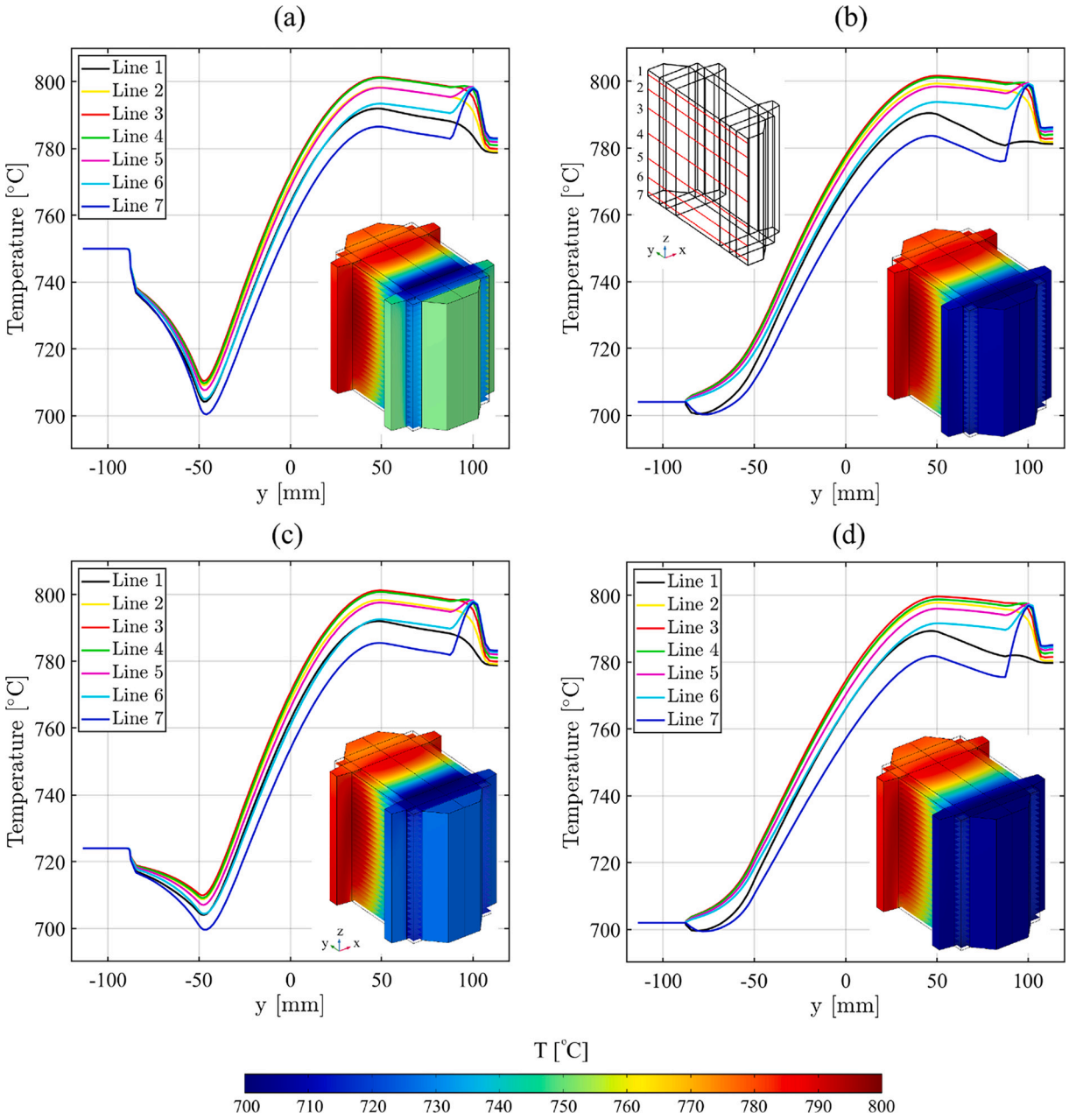

Fig. 5. Air temperature distribution inside the SOFC stack for different configurations (a) configuration 1 (0 % pre-crack, 0 % AOR), (b) configuration 2 (80 % pre-crack, 0 % AOR), (c) configuration 3 (0 % pre-crack, 70 % AOR), (d) configuration 4 (90 % pre-crack, 90 % AOR). Location of probe lines is shown in Fig. 5b.

Table 6
System outlet air temperature and system efficiency for different configurations.

Config	Case ID	System outlet air temperature [°C]	System efficiency [%]
1	0 % pre-crack, 0 % AOR	363	53.1
2	80 % pre-crack, 0 % AOR	274	51.6
3	0 % pre-crack, 50 % AOR	248	63.4
3	0 % pre-crack, 70 % AOR	192	69.7
3	0 % pre-crack, 90 % AOR	133	74.9
4	90 % pre-crack, 90 % AOR	71	72.0

3.2. Effect of steam content in AOR on the system performance

In the NH_3-fueled SOFCs, the outlet mixture of the SOFC stack contains N_2, H_2O, H_2 (due to fuel utilization factor being lower than 100 %), and possibly NH_3 (if there is any ammonia left uncracked which is not the case under the studied operating conditions). Despite the H_2, which is used in the SOFC after recirculation, N_2 and H_2O are not consumed and they accumulate inside the SOFC stack (see Table 3). Removing N_2 from AOR requires expensive membranes such as Palladium (Pd) membrane [40] and high power consumption is needed to separate N_2 from the anode off-gas. It was also shown in a recent study [14] that keeping the N_2 in the AOR loop reduces the output power of the cell negligibly. Hence, retaining N_2 in the AOR is practical from the system point of view.

On the other hand, steam (H_2O) content can be easily removed from AOR by cooling down the gas mixture and condensing the H_2O. The ratio of H_2O removal depends on the condenser which is considered to be 30 °C in this study which leads to removing around 95 % of steam content. However, the AOR mixture which is cooled down in the condenser (see Fig. 4c) should be heated up before feeding to the SOFC. This leads

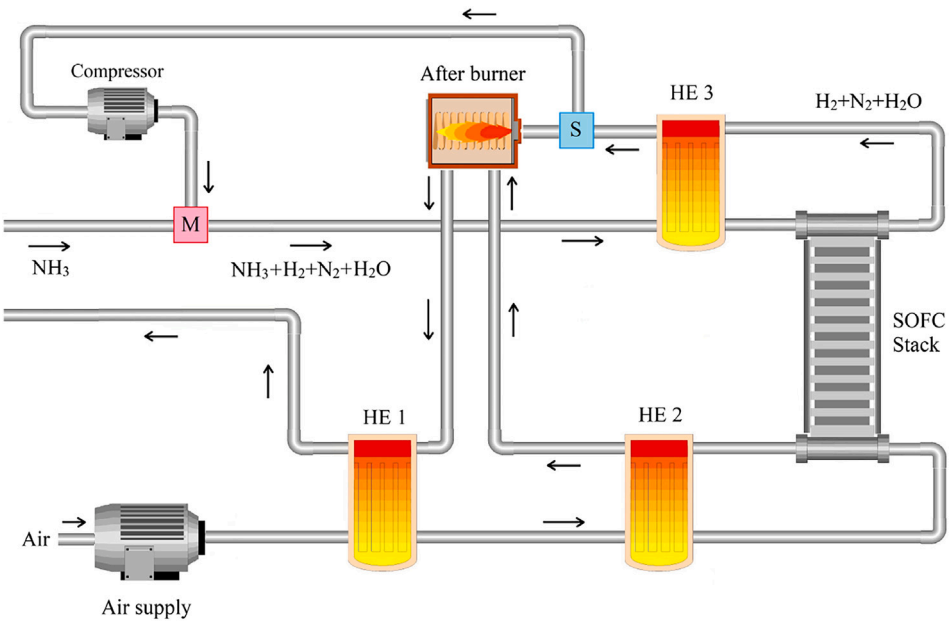

Fig. 6. Schematic of the configuration with AOR (configuration 3) considering the recirculation of steam content of the SOFC stack. In the schematic, heat exchangers are referred to as HE. S and M in the schematics represent splitter and mixer, respectively.

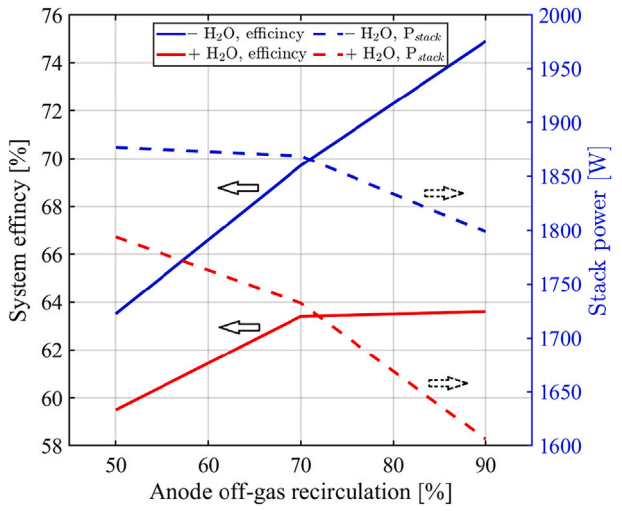

Fig. 7. Effect of anode off-gas recirculation (AOR) without steam (– H_2O) and with steam (+ H_2O) on the system efficiency and produced power of stack.

to some energy loss in the condenser. It is thus interesting to study the effects of keeping or removing the H_2O content in the AOR. In this section, configuration 3 which is the configuration with AOR is simplified by removing the condenser and a heat exchanger at the fuel inlet as shown in Fig. 6. The recirculated anode off-gas is mixed with the inlet ammonia to the system and the mixture containing H_2O is heated up in heat exchanger 3 (HE 3) to the inlet temperature of SOFC stack (700 °C).

Fig. 7 shows the effect of H_2O content in AOR on the system performance by comparing the system efficiency and stack power for the cases without steam (– H_2O) and with steam (+ H_2O). As can be seen, in the cases without steam (– H_2O), the stack power slightly reduces due to the delay in ammonia cracking and the dilution effect of nitrogen at high recirculation rates [14]. However, the system efficiency increases considerably (see Table 6) due to the reduction of the inlet molar flow rate of NH_3 into the system (Eq. (8)). On the other hand, for the cases with steam (+ H_2O) by removing the condenser (see Fig. 6), the stack output power reduces considerably due to the reduction of open circuit voltage with higher steam content [14]. Therefore, system efficiency is reduced considerably in the cases with steam (+ H_2O) compared to the cases without (– H_2O), which shows the importance of removing steam from the anode off-gas recirculation stream in the ammonia-fueled SOFCs. Therefore, in the final designed and selected system configurations in the next sections, approximately 95 % of the steam content is removed from the AOR using a condenser.

3.3. Nitriding risk for different system configurations

Direct utilization of ammonia in SOFCs also presents certain challenges in addition to its numerous advantages. Nitriding of nickel and steel is identified as one of the primary challenges in direct NH_3-fueled SOFCs. Hence, the potential for nitriding is examined across different system configurations. A qualitative validation of the Ni nitriding risk modeling approach was provided in a prior study, which focused on an NH_3-fueled SOFC at the cell level [14].

As described in the modeling section in the regions where $K_n/K_{n,cr}$ ratio has a value higher than 1, there is risk of Ni nitriding. Therefore, the distribution of the $K_n/K_{n,cr}$ ratio along a line passing through the middle of the SOFC stack in the flow direction is plotted for different configurations in Fig. 8a. The location of the line is shown in Fig. 8a. In this Figure, y = 0 cm depicts the center of the active area, y = −5 cm shows the region close to the inlet and y = 5 cm is the region close to the outlet. The region with Ni nitriding risk, characterized by $K_n/K_{n,cr} > 1$, is visually depicted as a red-shaded area.

Fig. 8a demonstrates that all cases and configurations that do not involve ammonia pre-cracking are susceptible to Ni nitriding. Under the studied operating conditions, it is necessary to implement nearly 90 % pre-cracking of ammonia in order to prevent Ni nitriding.

It is anticipated that the occurrence of Ni nitriding decreases as the amount of ammonia is reduced at higher anode off-gas recirculation (AOR) rates. Contrary to the expected trend, Fig. 8a reveals that an increase in the AOR rate actually amplifies the risk of Ni nitriding. By increasing the AOR rate, the fuel flow rate increases due to the accumulated nitrogen content in the AOR. This leads to a reduction in the residence time of NH_3 on the Ni catalyst and therefore, a reduction in

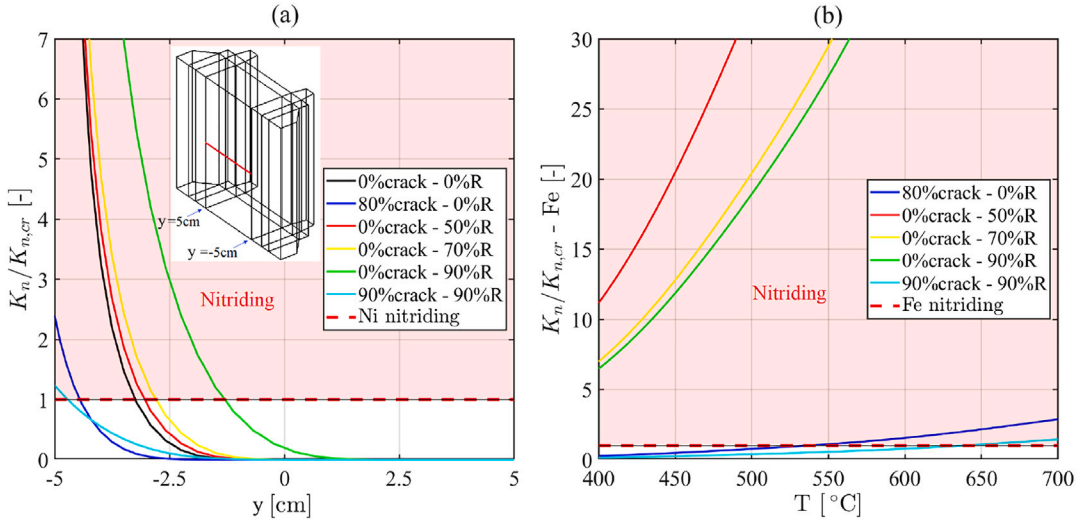

Fig. 8. (a) Comparison of ratios of $K_n/K_{n,cr}$ ratio in Ni layers for different configurations and (b) Comparison of ratios of $K_n/K_{n,cr}$ ratio for Fe in the steels in the system components such as pipes and heat exchangers considering no ammonia cracking on the steels. The red-shaded region shows the region with nitriding risk. In Fig. 8a, y = −5 cm and y = 5 cm represent the start and end of the active area, respectively. For the inlet and outlet of fuel flow see Fig. 3.

the ammonia cracking rate. The partial pressure (molar fraction) of ammonia also decreases by increasing AOR rate and increasing N_2 content which leads to the reduction of ammonia cracking rate (see Eq. (1)). This aligns with the experimental results reported in ref. [28], where it was observed that maintaining a constant ammonia flow rate while increasing the flow rate of Ar (as an inert gas) led to a decrease in the ammonia cracking rate. In the present study, N_2 serves as the inert gas. Furthermore, increasing the AOR rate increases the hydrogen in the SOFC inlet fuel stream, which reduces the ammonia cracking rate based on Eq. (1) and ref. [28]. As a result, increasing the AOR rate allows more ammonia to penetrate into the cell, which in turn accelerates the rate of nickel nitriding.

There is a high risk of nitriding of the steels in different components in ammonia-fueled SOFCs that may negatively affect the performance or the safety of the system severely. The nitriding has a tendency to weaken the metallic components, and if so this would cause cross over between air and fuel streams or probably even cause leaking of ammonia. Fig. 8b presents the $K_n/K_{n,cr}$ ratio for Fe considering no ammonia cracking on the steels in the system components such as pipes and heat exchangers. The red-shaded region shows the region with nitriding risk on Fe in pipes and heat exchangers by variation of temperature. The cases without ammonia pre-cracking exhibit a high risk of nitriding for steels. Therefore, the steel in the components should be protected by a coating to prevent nitriding.

Also in the previous study [27] it was shown that high thermal gradients in direct ammonia-fueled SOFCs will lead to higher thermal stresses than pre-cracked ammonia-fueled SOFCs that should be considered in the system design.

3.4. Sensitivity of the system efficiency to pressure drops

As previously mentioned, certain pressure drops are assumed for various components within the system (see Table 2). The pressure drop is known to be directly influenced by factors such as the design of components, the size and shape of channels in those components, and the flow rates. However, exact values for pressure drops need detailed information from the system components' designers which are not available. Therefore, a sensitivity analysis is conducted here to examine the importance of pressure drops on the overall efficiency and performance of the system.

In order to investigate the significance of pressure drops in the air side and fuel side separately, two distinct studies have been conducted,

Table 7
Various assumptions for pressure drops (ΔP) in the system components on the air and fuel side.

Pressure drop (ΔP)	Low guess [mbar]	Mid guess [mbar]	High guess [mbar]
ΔP heat exchanger air side	10	25	50
ΔP after burner air side	10	25	50
ΔP cracker air side	10	25	50
ΔP heat exchanger fuel side	5	12.5	25
ΔP cracker fuel side	5	12.5	25
ΔP condenser fuel side	5	12.5	25

Table 8
Sensitivity of the efficiency of the system to the pressure drops in the components on the air side of the system.

Pressure drop (ΔP)	Low guess	Mid guess	High guess
0 % pre-crack, 90 % AOR	74.9	73.6	71.6
90 % pre-crack, 90 % AOR	72.0	66.8	59.4
Efficiency reduction	2.9	6.8	12.2

where the pressure drops have been varied accordingly. In the first study, the pressure drop on the air side is intentionally increased, while maintaining a constant pressure drop on the fuel side, and vice versa in the second study. Table 7 displays various assumptions for the pressure drop on the air side and fuel side. This table represents the low guess (which is the assumed base pressure drop in Table 2), the mid guess, and the high guess for pressure drops.

The sensitivity of the system efficiency to the pressure drops on the air side is presented in Table 8. Only two configurations with a high AOR rate are presented and compared in Table 8. This is because as indicated in Table 6, a high AOR rate is required to attain a high system efficiency (>70 %). Table 8 provides clear evidence that the pressure drops on the air side have a substantial impact on the system efficiency. As it can be seen from Table 8, increasing the pressure drops considerably reduces the efficiency for the case including pre-cracking (90 % pre-crack, 90 % AOR). The main difference between the 0 % pre-crack, 90 % AOR case and 90 % pre-crack, 90 % AOR case is the difference in air flow rates in these cases. In the cases with pre-cracking, a higher air flow rate is necessary to effectively cool down the temperature of the SOFC stack, ensuring it remains within the range of 700–800 °C. Therefore,

Table 9
Sensitivity of the efficiency of the system to the pressure drops in the components on the fuel side of the system.

Pressure drop (ΔP)	Low guess	Mid guess	High guess
0 % pre-crack, 90 % AOR	74.9	74.0	72.8
90 % pre-crack, 90 % AOR	72.0	70.9	69.5
Efficiency reduction	2.9	3.1	3.3

Table 10
Sensitivity of the efficiency of the system to the pressure drops in the components on the fuel side of the system.

Pressure drop (ΔP)	Low guess	Mid guess	High guess
0 % pre-crack, 90 % AOR	74.9	73.6	71.6
90 % pre-crack, 90 % AOR – base case	72.0	66.8	59.4
90 % pre-crack, 90 % AOR – $T_{in,air}$ - 20 °C	73.4	69.7	63.0
Efficiency improvement by cooling air side	1.4	2.9	4.6

it can be concluded that the power consumption in the air supply unit considerably increases by increasing the air side pressure drops, which contributes to higher efficiency losses.

After performing a sensitivity analysis on the influence of the pressure drops on the air side, the effect of pressure drops on the fuel side of the system is investigated here. The sensitivity of the designed system efficiency to the pressure drops on the fuel side is presented in Table 9. The analysis reveals that the sensitivity of system efficiency to the pressure drops on the fuel side is lower compared to the sensitivity observed for the pressure drops on the air side. This discrepancy can be attributed to the fact that the fuel flow rate, even with a high AOR rate of 90 %, is generally much lower than the air flow rate. Consequently, increasing pressure drops have a relatively smaller impact on the power consumption of the recirculator than air supplier, resulting in a lower reduction in the system efficiency compared to the effect of increased pressure drops on the air supplier. However, there is still efficiency reduction by increasing the pressure drops on the fuel side which should be minimized.

3.5. Sensitivity of the system efficiency to air side inlet temperature

In this section, the impact of air side inlet temperature on the system efficiency is investigated, taking into account various assumptions for air side pressure drops. The objective is to understand how the variations in the air side inlet temperature affect the overall efficiency of the system under different configurations and pressure drops on the air side. Due to limitations on temperature variation within the SOFC stack, the air side inlet temperature is intentionally reduced by 20 °C in comparison to the fuel inlet temperature. This variation in air side inlet temperature is specifically implemented for the 90 % pre-crack, 90 % AOR case in order to explore the potential for improving the system efficiency through adjustments in the air side temperature.

The results of these two cases (with and without air side inlet temperature reduction) are compared with the 0 % pre-crack, 90 % AOR case results in Table 10 under varying air side pressure drops. The system efficiency shows significant improvement, particularly in high pressure drops, with the implementation of air side temperature reduction. The primary reason for this improvement is the reduction in air flow rate, which is necessary to control the maximum temperature of the stack. This reduction in air flow rate results in lower power consumption for the air supply, contributing to enhanced system efficiency.

4. Conclusion

In the current study, different system configurations are designed for ammonia-fueled SOFCs. The influence of the anode off-gas recirculation (AOR) and ammonia pre-cracking is investigated. Additionally, this study addresses nitriding of Ni and steel, which are key challenges in direct ammonia-fueled SOFC systems. A newly developed approach has been utilized as a design tool by integrating the system modeling with 3-D detailed multiphysics simulation to provide a better understanding of some of the main challenges of designing a durable and highly efficient ammonia-fueled SOFC system. All underlying physics, including electrochemical reactions, transport equations, heat transfer, and ammonia cracking reactions, are integrated to offer a detailed understanding of the ongoing processes. The key conclusions can be summarized as follows:

- For different system configurations, the air flow rate and inlet temperature should be adjusted accordingly to keep the temperature in the desired range (700–800 °C). For the case with 0 %, 50 %, 70 %, and 90 % AOR and without pre-cracking, the inlet temperature should be 750, 732, 724, and 718 °C for the studied cell materials and operating conditions.
- To achieve a high efficiency (η_I > 70 %) for the ammonia-fueled SOFC system, AOR should be implemented in the final system with a high recirculation rate. Considering 70 % fuel utilization for the SOFC stack and low pressure drops in the components of the designed system, the efficiency of the system for the cases with 0 %, 50 %, 70 %, and 90 % AOR rate and without pre-cracking are around 53 %, 63 %, 70 %, and 75 %, respectively.
- To prevent Ni nitriding in the cells of the SOFC stack under the studied conditions, approximately 90 % of the ammonia should be cracked prior to being fed into the stack, for the operating conditions of the considered stack technology. Therefore, an ammonia cracker should be included in the final system configuration with the chosen stack technology. The thermodynamic analysis revealed that there is a high chance of nitriding in steels in different components of systems. However, further experimental investigations are required to have a clear picture of nitriding on steels.
- Based on the results, the system with 90 % of ammonia pre-cracking and 90 % AOR is selected as the most efficient and durable system configuration.
- The sensitivity analysis of pressure drops indicates that the pressure drop in the air side components significantly affects the overall efficiency of the system, more so than the pressure drops on the fuel side. This effect is especially pronounced in configurations where ammonia pre-cracking is utilized, as a higher air flow rate is necessary to effectively cool the SOFC stack and keep it within the desired temperature range.
- It is important to reduce the pressure drops in the components of the system on the air side to reach an efficiency higher than 70 % for the system. According to the results, by increasing the pressure drops in the air side by a factor of 2.5 and 5, the efficiency of the system with 90 % pre-crack and 90 % AOR (which is the final selected configuration) will reduce by 6.8 % and 12.2 %, respectively compared to the base case with low pressure drops.
- Condensing the water steam out of the anode off-gas before recirculation is highly beneficial and increases the efficiency by around 10 %, as compared to keeping it in the recirculate, for the optimum recirculation conditions (90 % recirculation).
- The sensitivity analysis performed on the air inlet temperature of the SOFC stack shows that reducing the air inlet temperature can improve the system efficiency by reducing the air flow rate. This improvement is more profound in the cases with high pressure drop, resulting in a 4.6 % efficiency improvement compared to base case of 90 % pre-crack, 90 % AOR.

This study highlights the importance and efficacy of the developed coupled 3D/system modeling approach for simulating and designing

NH_3-fueled SOFCs, taking into account the complex multiphysics phenomena involved. The model can be employed to explore the performance and control of NH_3-fueled SOFC stacks and systems during load variations and dynamic operations.

CRediT authorship contribution statement

Arash Nemati: Writing – review & editing, writing – original draft, validation, software, methodology, investigation, and conceptualization. **Hossein Nami:** Writing – review & editing. **Javid Beyrami:** Writing – review & editing. **Rafael Nogueira Nakashima:** Writing – review & editing. **Henrik Lund Frandsen:** Writing – review & editing, supervision, resources, funding acquisition, and conceptualization.

Declaration of generative AI and AI-assisted technologies in the writing process

In preparing this work, the authors utilized chat.openai.com to check the grammar. Following the use of this tool, the authors reviewed and edited the content as necessary and take full responsibility for the publication's content.

Declaration of competing interest

The authors declare that they have no known competing financial interests or personal relationships that could have appeared to influence the work reported in this paper.

Acknowledgement

The authors sincerely appreciate the financial support received from the AMON project, which is funded by the Clean Hydrogen Partnership and its members, Hydrogen Europe and Hydrogen Europe Research, under grant agreement No. 101101521.

Co-funded by the European Union. Views and opinions expressed are however those of the author(s) only and do not necessarily reflect those of the European Union or the Clean Hydrogen Partnership. Neither the European Union nor the granting authority can be held responsible for them.

Supplementary material

Supplementary material to this article contains (A1) Ammonia cracking rate modeling and validation, (A2) Cell modeling and validation for hydrogen, pre-cracked and direct ammonia fueled SOFCs, as well as (A3) Stack level modeling and validation.

Supplementary data to this article can be found online at doi:10.1016/j.fuel.2025.134837.

References

[1] Zemp M, Huss M, Thibert E, Eckert N, McNabb R, Huber J, et al. Global glacier mass changes and their contributions to sea-level rise from 1961 to 2016. Nature 2019;568(7752):382–86.
[2] Fan L, Tu Z, Chan SH. Recent development of hydrogen and fuel cell technologies: a review. Energy Rep 2021;7:8421–46.
[3] Peng J, Huang J, Wu X-L, Xu Y-W, Chen H, Li X. Solid oxide fuel cell (SOFC) performance evaluation, fault diagnosis and health control: a review. J Power Sources 2021;505:230058.
[4] Cheng J, Lavery R, McCallum CS, Morgan K, Doran J, Wu C, et al. Crossflow flat solid oxide fuel cell (SOFC) semi-empirical modeling and the multi-fuel property based on a commercial 700 w stack. Fuel 2024;358:130172.
[5] Xu Q, Guo Z, Xia L, He Q, Li Z, Bello IT, et al. A comprehensive review of solid oxide fuel cells operating on various promising alternative fuels. Energy Convers Manag 2022;253:115175.
[6] Ong CW, Chang N, Tsai M-L, Chen C-L. Decarbonizing the energy supply chain: ammonia as an energy carrier for renewable power systems. Fuel 2024;360: 130627.
[7] Wan Z, Tao Y, Shao J, Zhang Y, You H. Ammonia as an effective hydrogen carrier and a clean fuel for solid oxide fuel cells. Energy Convers Manag 2021;228:113729.
[8] Hagen A, Caldogno R, Sun X. Direct ammonia sofc–a potential technology for green shipping. Fuel 2024;365:131238.
[9] Omer A, Rahimipetroudi I, Rashid K, Ullah KS, Kazmi WW, Kariim I, Hong JE, Dong SK. 10-cell direct ammonia solid oxide fuel cell stack design development with improved efficiency and resilience to thermal shock, Renewable Energy 2024; 121758.
[10] Hagen A, Langnickel H, Sun X. Operation of solid oxide fuel cells with alternative hydrogen carriers. Int J Hydrogen Energy 2019;44(33):18382–92.
[11] Trangwachirachai K, Rouwenhorst K, Lefferts L, Albanese JAF. Recent progress on ammonia cracking technologies for scalable hydrogen production. Curr Opin Green Sustain Chem 2024; 100945.
[12] Yang J, Molouk AFS, Okanishi T, Muroyama H, Matsui T, Eguchi K. A stability study of ni/yttria-stabilized zirconia anode for direct ammonia solid oxide fuel cells. ACS Appl Mater Interfaces 2015;7(51):28701–07.
[13] Kishimoto M, Muroyama H, Suzuki S, Saito M, Koide T, Takahashi Y, et al. Development of 1 kw-class ammonia-fueled solid oxide fuel cell stack. Fuel Cells 2020;20(1):80–88.
[14] Nemati A, Rizvandi OB, Mondi F, Frandsen HL. Detailed 3d multiphysics modeling of an ammonia-fueled solid oxide fuel cell: anode off-gas recirculation and ni nitriding degradation. Energy Convers Manag 2024;308:118396.
[15] Cinti G, Discepoli G, Sisani E, Desideri U. Sofc operating with ammonia: stack test and system analysis. Int J Hydrogen Energy 2016;41(31):13583–90.
[16] Rokni M. Addressing fuel recycling in solid oxide fuel cell systems fed by alternative fuels. Energy 2017;137:1013–25.
[17] Selvam K, Komatsu Y, Sciazko A, Kaneko S, Shikazono N. Thermodynamic analysis of 100% system fuel utilization solid oxide fuel cell (SOFC) system fueled with ammonia. Energy Convers Manag 2021;249:114839.
[18] Quach T-Q, Giap V-T, Lee DK, Israel TP, Ahn KY. High-efficiency ammonia-fed solid oxide fuel cell systems for distributed power generation. Appl Energy 2022;324:119718.
[19] Sun B, Xu Y, Liu Y, Ya Y, Cheng X, Quan Y, et al. Numerical design and evaluation of ammonia fueled solid oxide fuel cell (SOFC) power systems with different integration architecture: efficiency, power density and thermal safety. Energy Convers Manag 2023;298:117804.
[20] Cinti G, Liso V, Araya SS. Design improvements for ammonia-fed sofc systems through power rating, cascade design and fuel recirculation. Int J Hydrogen Energy 2023;48(40):15269–79.
[21] Quach T-Q, Lee D, Giap V-T, Kim YS, Lee S, Ahn KY. Energetic and economic analysis of novel cascade systems for ammonia-fed solid oxide fuel cell. Int J Hydrogen Energy 2024;67:1080–96.
[22] Wehrle L, Ashar A, Deutschmann O, Braun RJ. Evaluating high power density, direct-ammonia sofc stacks for decarbonizing heavy-duty transportation applications. Appl Energy 2024;372:123646.
[23] Meng T, Cui D, Shi Y, Ji Y, Cheng M, Tu B, Lan Z. Performance evaluation of high-efficiency sofc-pemfc hybrid system fueled by liquid ammonia. Int J Hydrogen Energy 2023;48(79):30887–30898.
[24] Qu J, Feng Y, Zhu Y, Wu B, Liu J, Jing H, et al. Thermodynamic analysis and comprehensive system optimization of the near zero emission hybrid power based on sofc-ice integrated system fueled with ammonia. Energy Convers Manag 2023;294:117553.
[25] Nemati A, Rizvandi OB, Nakashima RN, Beyrami J, Frandsen HL. Multiscale multiphysics modeling of ammonia-fueled solid oxide fuel cell: effects of temperature and pre-cracking on reliability and performance of stack and system. Appl Energy 2024;373:123913.
[26] Rizvandi OB, Miao X-Y, Frandsen HL. Multiscale modeling of degradation of full solid oxide fuel cell stacks. Int J Hydrogen Energy 2021;46(54):27709–30.
[27] Rizvandi OB, Nemati A, Nami H, Hendriksen PV, Frandsen HL. Numerical performance analysis of solid oxide fuel cell stacks with internal ammonia cracking. Int J Hydrogen Energy 2023;48(91):35723–43.
[28] Kishimoto M, Furukawa N, Kume T, Iwai H, Yoshida H. Formulation of ammonia decomposition rate in ni-ysz anode of solid oxide fuel cells. Int J Hydrogen Energy 2017;42(4):2370–80.
[29] Hendriksen PV, Mondi F, Sun X, Caldogno R, Frandsen HL, Rizvandi OB, et al. Ammonia as an sofc fuel. ECS Trans 2023) 2085;111(6).
[30] Fonović M, Leineweber A, Mittemeijer EJ. Experimental investigation and thermodynamic modeling of the ni-rich part of the ni-n phase diagram. Metal Mater Trans A 2014;45:4863–74.
[31] Wriedt H. The n-ni (nitrogen-nickel) system. Bull Alloy Phase Diagr 1985; 6(6):558–63.
[32] Kim S, Yoon S, Kim J-H, Park S. The effect of the transformation ofε-$Fe_{2-3}N$ into γ-Fe_4N phase on the fatigue strength of gas-nitrided pure iron. Metals 2020; 10(6):823.

[33] Alfano A, Puranen J, Pulkkinen V, Noponen M. Advancement on fuel and operation mode flexible solid oxide cell stacks and modules. In: EFCF; 2024.
[34] Navasa M, Miao X-Y, Frandsen HL. A fully-homogenized multiphysics model for a reversible solid oxide cell stack. Int J Hydrogen Energy 2019;44(41): 23330–47.
[35] Yu S, Zhang S, Schäfer D, Peters R, Kunz F, Eichel R-A. Numerical modeling and simulation of the solid oxide cell stacks and metal interconnect oxidation with openfoam. Energies 2023;16(9):3827.
[36] Nishida R, Beale S, Pharoah J, de Haart L, Blum L. Three-dimensional computational fluid dynamics modelling and experimental validation of the jülich mark-f solid oxide fuel cell stack. J Power Sources 2018;373:203–10.
[37] Kee R, Colclasure A, Zhu H, Kusnezoff M. Fuel cells – solid oxide fuel cell | cells and stacks. 2nd ed. Vol. 5. Elsevier; 2025. doi:https://doi.org/10.1016/B978-0-323-96022-9.00330-3
[38] Sekulic DP, Shah RK. Fundamentals of heat exchanger design. John Wiley & Sons; 2023.
[39] Weber M, Drobek M, Rebière B, Charmette C, Cartier J, Julbe A, et al. Hydrogen selective palladium-alumina composite membranes prepared by atomic layer deposition. J Memb Sci 2020;596:117701.
[40] Nordio M, Soresi S, Manzolini G, Melendez J, Annaland MVS, Tanaka DAP, et al. Effect of sweep gas on hydrogen permeation of supported pd membranes: experimental and modeling, Int. J. Hydrogen Energy 2019;44(8):4228–39.